A laser system for trapping and cooling of ^{6}Li atoms

by

Elmer Guardado-Sanchez

Submitted to the Department of Physics
in partial fulfillment of the requirements for the degree of

Bachelor of Science

at the

MASSACHUSETTS INSTITUTE OF TECHNOLOGY

June 2015

Author ... Signature redacted .....
Department of Physics
May 18, 2015

Certified by.. Signature redacted .....
Martin W. Zwierlein
Silverman Career Development Professor of Physics
Thesis Supervisor

Accepted by . Signature redacted .....
Nergis Mavalvala
Senior Thesis Coordinator

A laser system for trapping and cooling of ^{6}Li atoms

by

Elmer Guardado-Sanchez

Submitted to the Department of Physics
on May 18, 2015, in partial fulfillment of the
requirements for the degree of
Bachelor of Science

Abstract

In this thesis, I designed and built a laser system for the trapping and cooling of ^{6}Li atoms. The thesis starts explaining a theoretical background of the necessary laser frequencies for the realization of a Zeeman Slower and a 3D MOT. Next it describes the design of the laser system that makes use of a Raman Fiber Amplifier coupled with a Frequency Doubling Cavity and shows the finalized setup. Finally, the thesis delves into the topic of Modulation Transfer Spectroscopy which was used to lock the laser to the D_2 line transition of ^{6}Li and shows the spectroscopy setup built for the laser system.

Thesis Supervisor: Martin W. Zwierlein
Title: Silverman Career Development Professor of Physics

To my parents, Elmer and Hortensia

and my siblings...

Acknowledgments

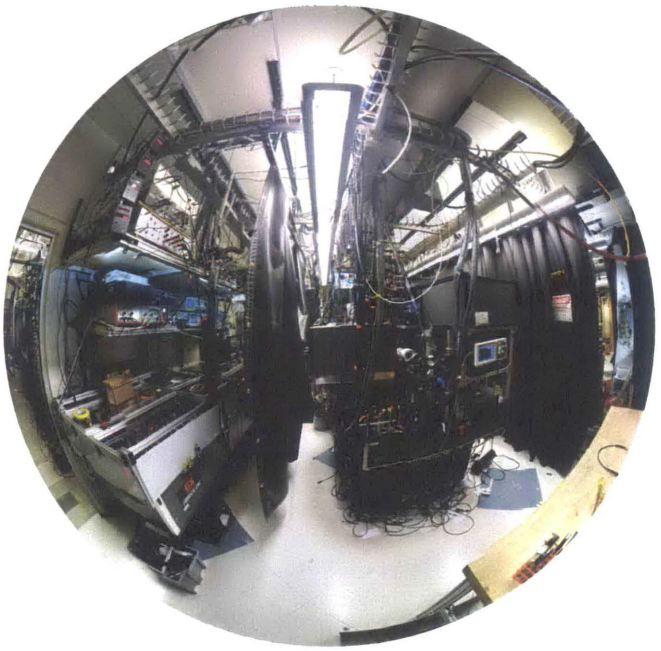

Figure 0-1: BEC1! Where chaos turns to beauty.

I was very lucky to have the opportunity to work in the BEC1 lab of the Zwierlein group along many great friends. From the very first time I met Martin Zwierlein I knew this was the group I wanted to join. Martin has taught me to love physics and be excited of even the simplest phenomenon. I thank him for all the effort he put into explaining the experiment to me. Many times a small question turned into a long discussion that ended sometime around 1am. But what I thank of him the most is his interest in helping me develop into a great scientist and person. I remember fondly many times where he picked me up for coffee to give me extensive advice about graduate school or explain why certain statements are not goosuitedd for a SOP. I thank him for being a mentor to me in and out of the lab, and I hope to make him proud on my future endeavors.

When I first joined the BEC1 lab, our post-doc Tarik Yefsah was the one that helped me understand all there is to know about an ultracold atoms lab. He knew that letting a sophomore hopelessly try to align a laser system for 5 hours only to have

him come and fix it in 5 minutes, was the best way to get me to learn. I thank him for always having a project for me to work on through my training. Also part of BEC1 was the now Dr. Mark Ku who always took time in the lab to answer my questions about the experiment. Biswaroop Mukherjee was a great colleague that never treated me like an "undergrad" for which I thank him a lot. Julian Struck was the second post-doc who joined the group; I want to thank him for all the patient explanations, for helping me build the laser system described in this thesis, and for being a friend. Wenjie Ji, Parth Patel, and Zhenjie Yan are the people who complemented my "BEC1" family.

In Fermi 1 and Fermi 2 where the rest of the people that made my experience incredible: Sebastian Will, Peter Park, Jenny Schloss, Zoe Yan, Emilio Pace, Thomas Lompe, Lawrence Cheuk, Melih Okan, Matthew Nichols, and Elizabeth Lawrence. Matt was always a great friend and his vast knowledge of Spanish baffled me at times. To Fermi 1: thanks for keeping a steady supply for my electronic boxes. To Fermi 2: thanks for having whatever I could not find in Fermi 1. To the entire group: thanks for making lunch breaks something to look forward to every day.

In the physics department I would like to thank Nancy Savioli for greeting me with a smile every time I visited the department. Christoph Paus showed me how to be an excellent experimental physicist and be relaxed at the same time; he was a great professor for Junior Lab. I thank my academic advisor Deepto Chakrabarty for trusting my ability to juggle the classes I took and giving me the best advice.

I specially thank Mark Belanger from the Edgerton Shop for teaching me the proper ways to machine pieces.

Outside of physics, I thank Sharanya Srinivasan for all her support and great patience when she helped me correct the hopeless grammar of the first draft of this thesis. I also thank the brothers at Theta Delta Chi for being my family at MIT. Finally, I want to thank my family for always believing in my and supporting my dreams. I thank my parents Elmer and Hortensia for making me the person I am today. I thank my siblings Claudio, Hortensia, Oscar Alfredo, and Mateo for making life fun and interesting before coming to MIT.

Contents

List of Figures

Chapter 1

Introduction

In the course of this thesis a laser system to trap and cool ^{6}Li atoms has been built. The setup will be part of a new apparatus for the creation of quantum degenerate fermions with tunable interactions in tailored optical potentials.

This new system is a direct upgrade to the one built by Z. Hadzibabic and M. W. Zwierlein, which is described in the doctoral thesis [9] and master thesis [25].

1.1 Motivation

A decade ago, the lab "BEC1" of Wolfgang Ketterle first demonstrated fermionic superfluidity and phase coherence of a ^{6}Li Fermi gas through the observation of a vortex lattice in the atomic cloud [24]. Most recently, the same experimental setup has been used to study solitary wave excitations in order to gain insight into many-body dynamics of fermions [23, 10].

Fermi gases are an interesting topic of research due to the possibility to discover new phases of nature that have yet to be theorized. Instead of trying to solve the system through theory, one can directly observe nature's behavior under different circumstances. Furthermore, ultracold Fermi gases are a well controlled system that is well suited to solve condensed matter problems through simulation. The laser system that is discussed in this thesis is meant to be part of a new laboratory that will study an even wider range of quantum systems. This lab will be a "reloaded" version of

BEC1. This new lab will initially focus its efforts in homogeneous trap potentials to effectively simulate the behavior of many interacting fermions in a box and the different phases that they can reside in. This new experiment will again use ^{6}Li to generate a Fermi gas, which needs a 671 nm wavelength for all the experimentally important transitions.

1.2 Properties of our laser system setup

The laser system uses a 1342 nm laser diode that is amplified to 5 W using a Raman Fiber Amplifier from the company MPB Communications Inc. This beam is then passed through a frequency doubling cavity from the Italian company LEOS^{TM} that outputs a 671 nm laser beam with 1.6-1.8 W power. This is more than enough to generate all the needed frequencies for the system and it is the main property of our setup that differentiates it from previous systems such as [9, 25].

Another important property is the method used to lock the laser to the D_2 line transition. We use Modulation Transfer Spectroscopy (or Four-wave mixing) to generate an error signal that has several advantages compared to other schemes.

There are other small optimizations of which only one is worth mentioning. The light that goes through the ^{6}Li vapor cell in the spectroscopy setup is offset by +228MHz in order to have the main locked beam offset -228MHz from the D_2 line transition and minimize the Acousto-Optic Modulators (AOMs) needed in the laser system to generate all required outputs.

1.3 Outline of this thesis

The purpose of this thesis is to serve future students in the Zwierlein Group. Therefore, the following chapters are going to explain both the theoretical knowledge needed to understand the system and the technical specifics of it. This should provide enough background for any student to fully comprehend this experimental tool.

The chapters are organized as follows:

Chapter 2 presents the theory behind the trapping and cooling of ^{6}Li atoms. We will present the structure of ^{6}Li and relevant transitions in it.

Chapter 3 shows the actual laser setup that was built. It will describe how each part and component serves to produce all the desired outputs.

Chapter 4 focuses on the Modulation Transfer Spectroscopy (MTS); first describing the theory behind this method and then showing the implementation of it in our setup. It will also focus on the electronic components of the setup.

The Appendix A provides a guide to build an Electro-Optical Modulator as the one that was used for spectroscopy in this laser system.

Chapter 2

Understanding laser trapping and cooling of ^{6}Li atoms

This chapter will present the theoretical background to understand the laser system. It is divided in three main sections. The first section discusses the properties of ^{6}Li atoms, their intrinsic constants, and their transitions. The second section explains the mechanism by which a laser beam exerts a force on an atom and how to apply this force to slow down atoms in a Zeeman slower. The third section deals with the problem of trapping and cooling the atoms using a Magneto-Optical Trap (MOT). Finally, we briefly address the part of the system that will be used for absorption imaging.

2.1 Properties of ^{6}Li and its structure

Lithium belongs to the family of alkali atoms which are characterized by a single valence electron and makes them a relatively easy model to do quantum science. For optical transitions only this valence electron is relevant and all alkali atoms share a similar level structure where the transition from $nS_{1/2}$ to $nP_{3/2}$ (D_2 line) is most commonly used for cooling and trapping. Lithium is usually found in mixtures of two isotopes: 92.5% bosonic ^{7}Li and 7.5% fermionic ^{6}Li [7]. In fact, ^{6}Li is one of the only two stable fermionic isotopes of alkali atoms, the other one being ^{40}K [17].

The electronic structure of the ground state of Lithium is $1s^2 2s^1$. This means that in ^{6}Li the ground state is equal to having the external electron in the orbital state $2S_{1/2}$. The first excited states of any alkali atom are split into the fine structure due to the coupling of the electron's spin (S) and orbital momentum (L) into states $nP_{1/2}$ and $nP_{3/2}$. The notation used in these excited states defines the subscript as the quantum number J associated with the total angular momentum of the electron $\vec{J} = \vec{L} + \vec{S}$. The energy differences between each excited state and the ground state is the reason for the spectral D lines at 671nm[1]. For laser cooling, we use the D_2 line transition that links the ground state with the $nP_{3/2}$ state. In the case of ^{6}Li $n = 2$.

Furthermore, there is a hyperfine splitting that affects both the ground and excited states. This splitting is due to the coupling between the total angular momentum (J) and the nuclear spin (I). For small magnetic fields, the quantum number F associated with $\vec{F} = \vec{J} + \vec{I}$ is a good way to describe each of the split states. For ^{6}Li the nuclear spin is $I = 1$ and causes a splitting of 228 MHz in the ground state [9]. The states with highest quantum number F in the ground state ($F = 3/2$) and excited $2P_{3/2}$ state ($F' = 5/2$) form a "cycling transition" which emulates a two-level system. Figure 2-1 shows the energy level structure of ^{6}Li with the relevant transitions for laser cooling.

2.2 Slowing atoms

Cold atom experiments start with an atomic beam emanating from an oven and slowed down through a Zeeman slower [14] to reach a speed that can be trapped inside a MOT [15]. It depends on the species: for Lithium or Sodium it is necessary, but other species such as Rubidium do not need to be slowed in order to be trapped. Lithium has to be heated to around 400°C in order to melt and generate enough vapor pressure to generate a high-flux atomic beam. In order to understand how the Zeeman Slower works, it is important to first conceptualize the force that a laser beam exerts on an atom.

[1] The D lines correspond to the transition from the ground state to each of the two excited states

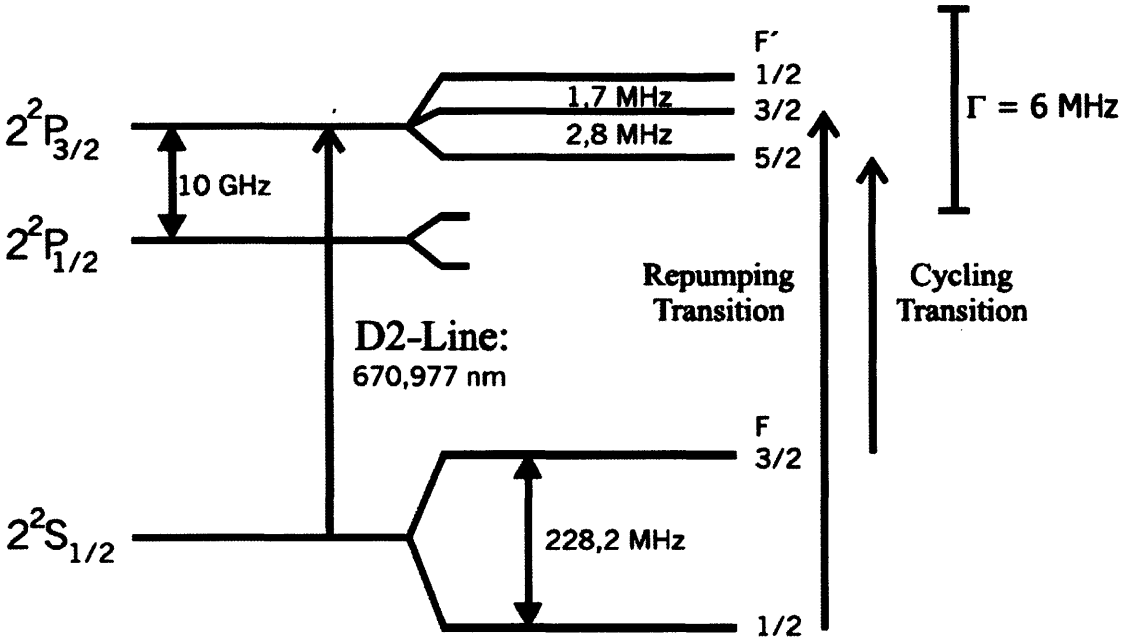

Figure 2-1: Energy level structure for laser cooling of ^{6}Li. Figure adapted from [25].

2.2.1 Laser forces on an atom

The ability to exert forces on atoms and thus manipulate them is one of the principal tools that a physicist uses to perform experiments in an ultracold atoms lab. By shining a laser beam on to an atom, it is possible to impart a force in the same direction of the laser beam. Since the scope of this thesis is only to present enough knowledge to understand these processes, a full calculation of this force will not be made. A detailed derivation of this force can be found in [8].

Let us take into account a laser beam with frequency ω and momentum $\hbar\vec{k}$ that is directed onto an atom, modeled as a two-level system with energy difference $\hbar\omega_0$. Here, we can describe the strength of the effect that the laser has in the atom by the saturation parameter $s = 2\Omega_R^2/\Gamma^2$, where Ω_R is the Rabi frequency[2] and Γ the linewidth of the transition between the ground and excited states[3]. A final important

[2]The Rabi frequency is the frequency of oscillation between two atomic states inside a light field. It is defined as $\hbar\Omega_R = d_{i,j} \cdot E$, where $d_{i,j} = \langle i| d |j\rangle$ is the matrix element of the electric dipole operator between the two states and E is the electric field of the laser beam.

[3]This linewidth defines the characteristic time $T = 1/\Gamma$ over which an excited state will spontaneously emit a photon and decay.

value is the detuning of the laser $\delta = \omega - \omega_0$; positive detunings are called "blue" and negative detunings are called "red" making allusion to Doppler shifts. With these concepts in place it is now possible to understand the formulas governing the light force.

When the laser beam is shining on the atom, the atom is going to absorb a near-resonant photon and transition into the excited state. In doing so, the atom will also absorb the momentum that the photon carried and get a kick in the direction of the laser beam. After a time defined by the inverse linewidth Γ^{-1} this atom will spontaneously emit another photon and receive another kick; however, this time the photon has equal probability to be emitted in opposite directions. Over a large amount of absorption and emission processes, the average change in momentum due to the spontaneous emission will cancel out. Therefore, the atom is effectively being pushed in the direction of the laser beam. The effective force will then be given by the rate of absorbed photons times and the imparted momentum per photon. The scattering rate depends on the linewidth of the transition, the detuning, and the saturation parameter:

$$\vec{F} = \hbar\vec{k}\gamma_s = \hbar\vec{k}\frac{\Gamma}{2}\frac{s_0}{1 + s_0 + (2\delta/\Gamma)^2} \tag{2.1}$$

In the case of ^{6}Li: the natural linewidth is $2\pi \times 6$ MHz, the laser intensity in order to get $s_0 = 1$ is 2.5 mW/cm^2, and the recoil velocity $v_{rec} = \hbar k/m$ is about 10 cm/s [9]. The saturation intensity sets a natural scale for the required beam intensity. In general, it is favorable to work with high saturation parameters in order to be insensitive to power fluctuations and changes.

2.2.2 The Zeeman Slower

In the calculations above, we omitted certain effects that can also affect the detuning of the laser. One of these effects is the Doppler shift. When the atoms leave the oven, they are moving at a fast velocity that can be calculated by the formula:

$$v_{th} = \sqrt{2\frac{k_B T}{m}} \tag{2.2}$$

This formula represents the most probable speed in a thermal distribution corresponding to the temperature T of the oven. In the case of ^{6}Li coming out of the oven at a temperature of 400°C, this speed is $\approx$ 1270 m/s. In this condition, the frequency that the atoms "see" will be Doppler-shifted, therefore affecting the detuning of the laser with the transition. The Doppler shift adds a term $-\vec{k} \cdot \vec{v}$ to the detuning δ used in Equation 2.1. In this case, the Doppler shift corresponds to $2\pi \times 1.8$ GHz between atoms leaving the oven and atoms at rest.

Another possible shift in the detuning is due to the Zeeman Effect. We can connect the cycling transition of ^{6}Li using a laser beam with σ^- polarization[4] due to selection rules. These states have such quantum numbers that at any external magnetic field, the ground state has magnetic moment equal to one Bohr magneton μ_B and the excited state equal to $2\mu_B$. Therefore the total Zeeman shift of the transition is $-\mu_B/h = -1.4$ MHz/G [9]. This generates a modifying term to δ equal to $+B(\vec{r})\mu_B/h$.

The Zeeman slower is then used to counterbalance the unavoidable Doppler shift due to the fast atoms, using a tailored magnetic field [14]. This allows the slowing of the atoms using a laser beam with static frequency by balancing out the Doppler and Zeeman shifts (hence the name). The total detuning has the form:

$$\delta(\vec{v}, \vec{r}) = \omega - \omega_0 - \vec{k} \cdot \vec{v} + B(\vec{r})\mu_B/h \tag{2.3}$$

In the experiment, the Zeeman Slower is built such that the detuning is kept constant to maximize the constant slowing of the atoms to a speed that can be trapped using a MOT. A final detail to take into consideration for the experimental realization of the Zeeman slower is that the atomic beam of ^{6}Li comes out both in the $F = 3/2$ and $F = 1/2$ states of the ground state. It is necessary to send, along the

[4] $\sigma^\pm$ denotes circularly polarized light where + means clockwise and - counter-clockwise- with respect to the direction of propagation.

slower beam that drives the cycling transition, a "repumping" beam detuned +228 MHz from the slower beam so that it takes the lower hyperfine state to the upper state through the repumping transition.

2.3 Trapping atoms in a MOT

With the atoms slowed down, it is possible to trap them using a different array of the same light forces. In a MOT, there are two force components that allow it to both spatially trap the atoms and cool them. The damping or cooling term will be addressed first.

2.3.1 Doppler Cooling

Knowing that a laser beam can exert a force on an atom in the same direction it is propagating, it is a logical step to think that it is possible to trap atoms in between two counter-propagating laser beams. However, if the frequency of the laser beams was exactly that of the cycling transition the forces would effectively cancel out. An easy way around this dilemma is to have the laser beams red detuned below the cycling transition frequency. The reasoning is that since atoms are moving at some speed v, we can exploit the Doppler shift to the laser detuning in order to make one of the forces stronger than the other one.

In the case of the beam propagating against the direction of the atom, the Doppler shift will reduce the magnitude of the detuning, hence increasing the magnitude of the force it imparts. Conversely, the other beam will be shifted furthera way from the transition reducing the force it generates on the atom. This way, there will be a force term of the form $F_{\text{cooling}} = -\alpha\vec{v}$ in the direction of the axis that the two beams propagate in. An actual calculation of the constant α using Equation 2.1 can be found in [8].

To make a full 3D construction using this technique, we need 3 pairs of counter-propagating red detuned laser beams in 3 perpendicular axis. However, the force that the atoms feel is not a spatial confinement, but rather a damping or viscous term.

The atoms will move in a random walk as if immersed in a viscous liquid which is why this is usually referred to as an "optical molasses" [7].

Although the atoms will not be trapped, they will cool down due to the damping. The minimum temperature at which these atoms can be cooled down in this simplified system is defined by $k_B T_{\text{Doppler}} = (1/2)\hbar\Gamma$. For ^{6}Li, this temperature is 140μK [9].

2.3.2 Magneto-Optical Trap

In order to generate a spatial confinement we need to add a magnetic field gradient to the optical molasses. Thereby, we exploit the atom's internal structure to increase the absorption of light near the center of the trap [15].

For a simple case, let us imagine a 1D-MOT in the z axis and an atom with $J = 0$ in the ground state and $J = 1$ in the excited state. The magnetic field has the form $B_z = bz$ and generates a Zeeman shift of the energy level with value $\Delta_{\text{Zeeman}} = \mu m_s B$. Here, m_s is a quantum number that can have values {+1,0,-1} in this simplified system. In a MOT, the polarization of the counter-propagating beams is very important. The beam propagating in the positive z direction needs to have polarization σ^+ while the other beam needs polarization σ^-. These polarizations are important because due to the selection rules, σ^+ polarization can only excite the ground state to the $m_s = +1$ state and σ^- only to the $m_s = -1$ state. Figure 2-2 shows the case explained above.

Due to the selection rules of the counter-propagating beams, there will be a force on the atoms that always points to the center of the trap. This force will have the form $F_{\text{confinement}} = -\beta z$ and it is the spatial confinement term that along the damping term traps the atoms. A full 3D-MOT will have 3 pairs of counter propagating beams with $\sigma^{\pm}$ polarizations in 3 perpendicular axis. The point where they meet will be at the center of a "spherical quadrupole" magnetic field that can be generated using a pair of anti-Helmholtz coils. This configuration is shown in Figure 2-3.

The MOT is the first step towards experimentation in ultracold atoms. While it does not cool down the atoms to degeneracy, it does localize them at a cold enough temperature and with enough density to use further processes like evaporative cool-

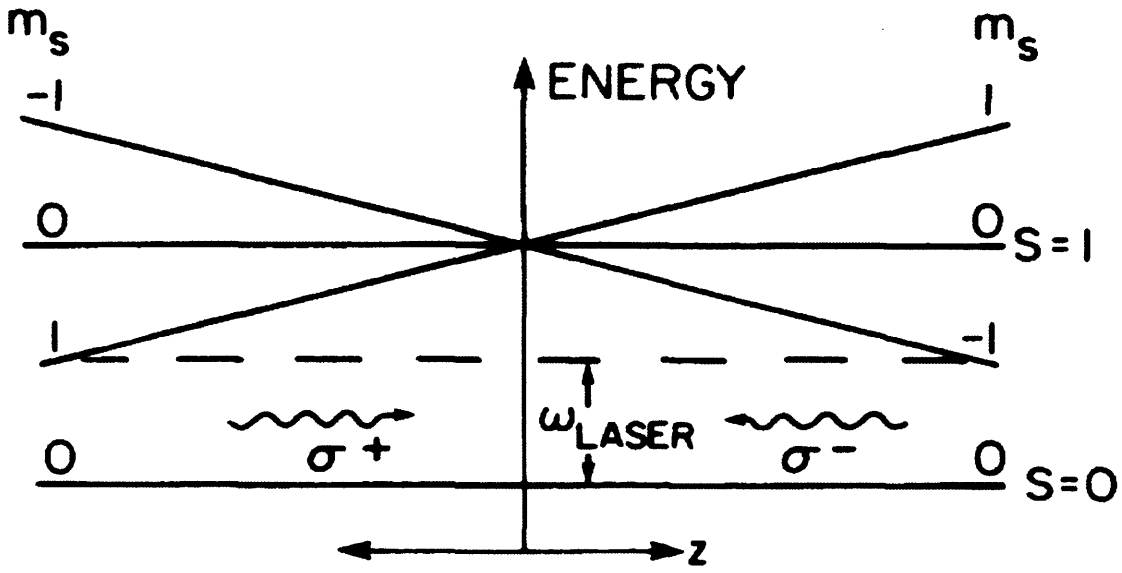

Figure 2-2: Energy level diagram of an atom in a 1D-MOT. Due to the selection rules of the polarized counter-propagating beams, there will be a light force pointing towards the zero crossing of the magnetic field at $z = 0$. Figure taken from [15].

ing. Similar to the slower process, for the MOT trap to work correctly, we need a repumping frequency along the red detuned cycling transition one. This frequency will not be red detuned from its transition, but it is necessary for a working MOT by keeping all the atoms in the cycling transition.

2.4 Imaging

A final topic that is important for the laser system built for this thesis is the imaging of the atoms. For this process, we need a mixture of the cycling and repumping transition frequencies[5]. These are not detuned at all from their respective transitions and can be used to perform many kinds of imaging schemes. The two most widely used are absorption and fluorescence imaging. This thesis will not present the background for these schemes, but there are many good sources out there including [13].

[5]This will only work in the low magnetic field regime. For high magnetic field imaging, an offset is needed due to the Zeeman effect where F is no longer a good quantum number.

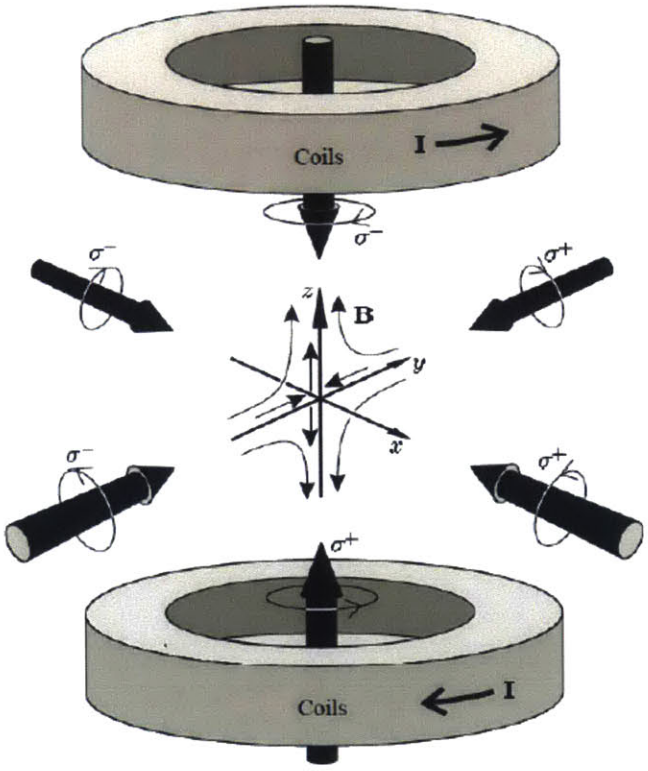

Figure 2-3: 3D-MOT configuration using a pair of anti-Helmholtz coils. Figure taken from [5].

Chapter 3

Laser system

This chapter will present how the laser system was built. It starts with an outline of the different frequencies that need to be generated. Next it will delve into how we generate a high power 671 nm laser source using a Raman Fiber Amplifier (RFA) and a frequency doubling cavity. Then, we will explain how to offset the frequency of the laser beam using Acousto-Optic Modulators (AOMs) and their different possible configurations. With this knowledge, we explain how the laser system was designed to give the necessary outputs. Finally, we show the layout of the laser system that was built.

3.1 Outline of the system

In order to build a laser system that allows for the slowing, trapping, and initial cooling of ^{6}Li we need very specific frequency outputs as Chapter 2 suggests. There are 3 main outputs that we need from the laser system:

1. **Slower + Repumper.** 1 GHz red detuned light from the cycling transition between the $F = 3/2$ ground state to the $F = 5/2$ excited state. Plus, 1 Ghz red detuned light from the repumping transition[1] between the $F = 1/2$ ground state to the $F = 3/2$ excited state (or 228 MHz blue detuned from the Slower

[1] Refer to Figure 2-1.

light). The offset of 1Ghz red detuned light is in the magnitude of the typical Doppler shift for ^{6}Li atoms out of the oven.

2. **MOT + Repumper.** 20MHz red detuned light from the cycling transition between the $F = 3/2$ ground state to the $F = 5/2$ excited state. Plus, light exactly resonant with the repumping transition between the $F = 1/2$ ground state to the $F = 3/2$ excited state. The detuned frequency of the MOT signal generates the damping force that cools the atoms while also spatially trapping them.

3. **Imaging.** Resonant light with the cycling transition between the $F = 3/2$ ground state to the $F = 5/2$ excited state. Plus, resonant light with the repumping transition between the $F = 1/2$ ground state to the $F = 3/2$ excited state. These frequencies will only work for the low-field imaging.

In order to generate all these outputs, we first need to know how to get enough laser power at 671 nm. Furthermore, this beam will be divided into three main lines and offset using Acousto-Optic Modulators (AOMs). The next sections will explain the steps in the laser system that eventually end up with the desired outputs and finally show a layout of the laser system that was built.

3.2 Generating a powerful 671 nm source

Since there are not many viable commercial options for a high power 671 nm laser, we opted to buy a 1342 nm diode laser, amplify it using a Raman fiber amplifier, and halve its wavelength using a frequency doubling cavity. We will briefly describe each of these components, how they work, and their important attributes for the experiment.

3.2.1 1342 nm Master Laser

The diode laser used is a Toptica^{TM} DL Pro laser. This laser has a linewidth below 1MHz which is better than what we need for ^{6}Li. The spectroscopy and locking of

the laser will be addressed in Chapter 3. However, for this chapter it is important to know that laser will be locked so as to have a frequency 228 MHz red detuned from the cycling transition.

The laser is run at a driving current of 110-120 mA in order to have an output of ~30 mW. This is the minimum output required for the Raman fiber amplifier to saturate. By driving the laser with the minimum current possible we ensure the maximum lifetime of the diode.

3.2.2 Raman Fiber Amplifier

We use a commercially available Raman fiber amplifier from the company MPB Communications Inc. This amplifier takes in an input of 26.5 mW @ 1342 nm (after a ~80% fiber coupling) and gives out a beam of 5 W at the same wavelength through a fiber. The process by which this amplifier works is Stimulated Raman Scattering (SRS).

Stimulated Raman Scattering

In this thesis we will only present a simple intuitive model for SRS. For a full calculation of the results, consult Chapter 4 of [20]. The Raman Fiber Amplifier works using two input signals: a seed beam (the 1342 nm light in our case) and a high-power (10 W) pump beam 1100 nm from an Ytterbium Fiber Laser. Through a non-linear interaction with the fiber medium, the atoms generate a vibrational state that favors the inelastic scattering of the 1100 nm light into the 1342 nm light by a two photon process. Since the 1100 nm light is shifted to a higher wavelength, this is called a Stokes shift [18]. Figure 3-1 shows an energy level diagram of this process. The seed beam gets amplified by transforming 1100 nm light to 1342 nm light in this second order process.

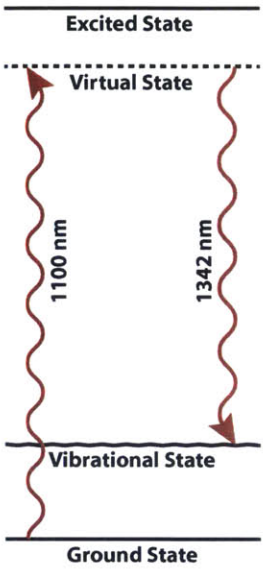

Figure 3-1: Energy level diagram of the Stimulated Raman Scattering process inside the Raman Fiber Amplifier.

Raman Fiber Amplifier to produce a 671 nm source

Using Raman Fiber Amplifiers (RFAs) in conjunction with a frequency doubling cavity to generate a high power laser beam in the 550 to 700 nm region was pioneered by [22]. This group originally developed this method to generate a 25 W @ 532 nm laser beam to use in astrophysics as a star tracking tool.

3.2.3 Frequency Doubling Cavity

The frequency doubling cavity was bought form the Italian company Laser and Electro-Optic Solutions (LEOS). This cavity is similar to the ones employed by the group of Gabriele Ferrari [11]. Given an input of 1342 nm light the cavity generates an output of 671 nm light as desired.

The cavity uses a $KNbO_3$ non-linear crystal that doubles the frequency of the incident light by Second Harmonic Generation. It amplifies this effect using a high finesse bow-tie cavity which ultimately transforms an input of 5W @ 1342nm light to 1.6-1.8W @ 671 nm. This output is more than enough to generate all the desired outputs with power to spare.

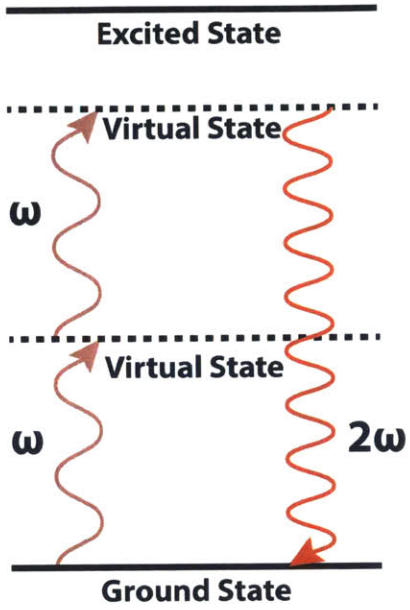

Figure 3-2: Energy level diagram of the Second Harmonic Generation. Note how the frequency of the emitted light is twice of that of the absorbed light.

Second Harmonic Generation

In 1961, a group led by Peter Franken at the University of Michigan, Ann Arbor first demonstrated that light could be converted into a different color though a non-linear effect [6]. In their experiment, they shone a 694 nm laser through a quartz sample and measured the spectrum of the output. This measurement showed a small amount of 347 nm light which was famously mistaken by the PRL editor as a speck of dust and subsequently erased from the published paper.

The full calculations that arrive at the theoretical solution of Second Harmonic Generation can be found in [3]. However, it can be understood in a simple intuitive way. If the atoms in the crystal are in their respective ground states. The frequency gets doubled by a two-photon process where two photons get absorbed so that the atom gets excited through a virtual state to another and from this final excited state the atom decays back to the ground state emitting only one photon. Since it absorbed two photons and emitted only one, this output photon has double the input frequency to preserve energy conservation. Figure 3-2 shows a diagram of this process.

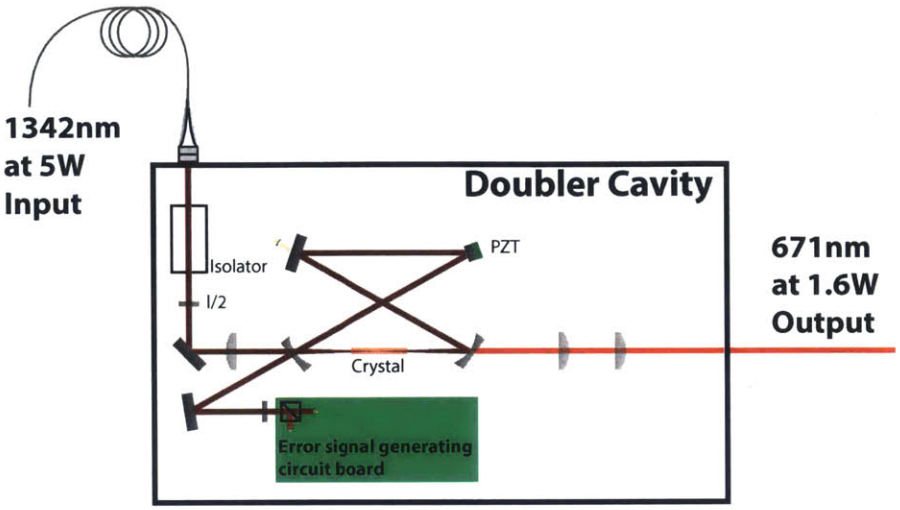

Figure 3-3: Schematic of the inside of the frequency doubling cavity.

Locking the cavity

The cavity comes with its own temperature controller for the crystal and PID box to lock the cavity. Figure 3-3 shows a schematic of the inside of the doubling cavity. One of the four mirrors in the cavity has a small piezoelectric transducer (PZT) that can fine tune the cavity until it is resonant. This particular cavity was very difficult to lock at the beginning. Due to some errors, we had to re-align the whole optical setup inside the box and replace the optical isolator. We also needed to modify the values of the attenuators before the polarizing beam splitter cube that generated the signal for the polarization spectroscopy and with that generated an error signal. Finally we changed the potentiometer from the Integral gain in the PID box.

3.3 Generating the different frequencies

In this laser system, we only use AOMs to modify the frequencies of the beams. AOMs allow us to add or substract an offset on the order of magnitude of hundreds of MHz to any incident laser beam and also separate the part of the beam that got offset from the one that did not.

3.3.1 Acousto-Optic Modulation of Light

An AOM consists of a transparent crystal (TeO_2 in the case of this laser system) which is being vibrated by a RF driven PZT from one side and has damper on the other. This causes the continuous generation sound waves or phonons that only travel in one direction. In this laser system, the PZT is driven with home-built drivers at the specific frequencies that we want to offset the laser. A design for these drivers is in [25] and also in [17].

When a laser beam is sent perpendicular to the direction of the phonons inside the crystal, there is an interaction between the photons and the phonons. There are three main possible effects:

1. The photon passes unscattered through the crystal.

2. A phonon is absorbed by the photon receiving both its energy (positive frequency shift) and its momentum (positive spatial shift).

3. A phonon is emitted by the photon losing both some energy (negative frequency shift) and momentum (negative spatial shift).

Figure 3-4 shows all three of these processes. In reality, even higher order shifts are present. The efficiency at which the power of the light is distributed between the possible outputs depends strongly in the incident angle, beam size, and polarization. This is why we put a telescope before almost every AOM in the laser system. The normal efficiency for a first order diffraction in a $\sim$100 MHz driven AOM is $\sim$85%, for $\sim$200 MHz its $\sim$75%, and for $\sim$300 MHz its $\sim$70%. A more comprehensive description of the way an AOM works is calculated in [17].

3.3.2 Double-Pass AOM

A Double-Pass AOM means that the diffracted light is retro-reflected back exactly in the same direction. By doing this, the zeroth order diffraction will not have any change but loss of power due to the efficiency of the alignment. On the other hand,

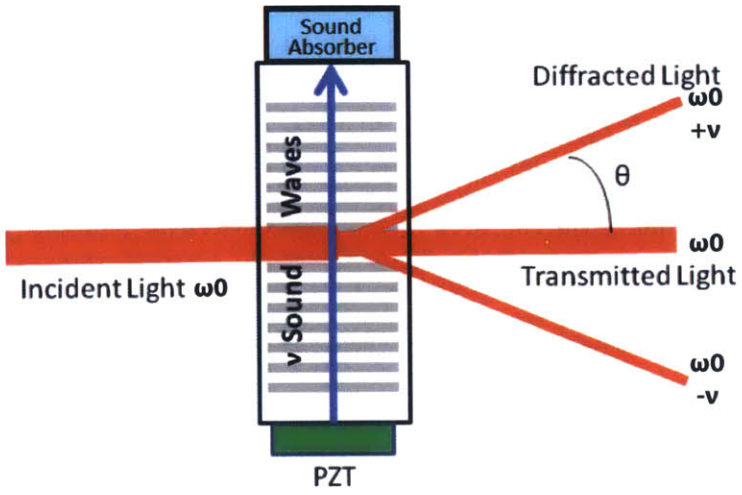

Figure 3-4: Diagram of how an Acousto-Optic Modulator works. The incident light either passes by normally, absorbs, or emits a phonon. Figure adapted from [17]

the first order diffractions will have double the offset and return in the exact same direction as they came. The normal way to set a Double-Pass AOM is to put a lens at a distance equal to its focal length from the center of the AOM. This way all diffractions can be retro-reflected together in the same mirror. However, this presents a problem of superimposed beams coming in and out of the AOM. Going in is the original beam with frequency ω; and going out is a mixture of ω and the doubly offset beams of the diffractions. A easy way to separate them is to make use of a Polarizing Beam Splitter (PBS) and placing a quarter wave-plate before the mirror[2]. This way the out coming light will go in the opposite output of the beam splitter as it will have the opposite linear polarization as the incoming beam. Figure 3-5 shows a basic setup for a Double-Pass AOM.

It is important to note that the efficiency of a Double-Pass AOM is calculated as the square of the efficiency of a single-pass AOM driven at the same frequency.

[2]All throughout the Laser system the beams are linearly polarized unless we use quarter wave plates to make then circularly polarized. In this case, by placing a quarter wave plate right before a retro-reflecting mirror you ensure that the incoming and out coming beams have opposite linear polarization.

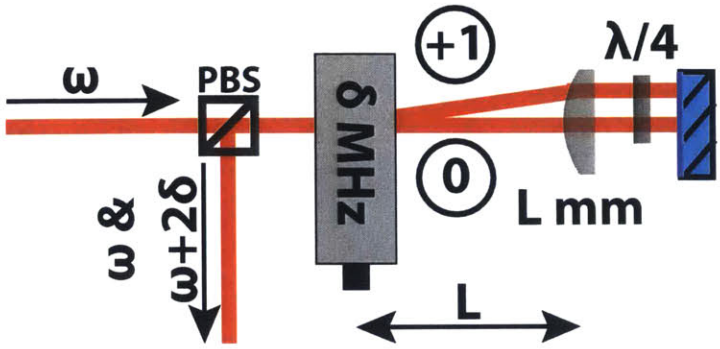

Figure 3-5: Double-Pass AOM basic optical setup. The circled numbers mark which diffraction beam from the AOM it is. It clearly shows the output being a mixture between two beams, one with the input frequency and one doubly offset. By simply blocking the zeroth order diffraction beam we would only have the doubly offset beam output.

3.4 Design of the laser system

In this section, each part of the finished laser system is explained. Having explained the different ways to offset the frequency of a laser beam, this section provides the process in which each output is generated without going into the specifics of the setup. This can be seen as the "topology" of the laser system.

3.4.1 Spectroscopy and Generation of the Main beam

As explained in past sections: 1342 nm laser light comes out of a laser and is amplified through a Raman Fiber Amplifier (RFA) to then be converted into 671 nm amplified light in a frequency doubling cavity. After this process generates the main laser beam of the setup, a little bit of light is taken to do spectroscopy and lock the laser 228 MHZ red detuned from the cycling transition. The rest of the light is divided for the other three parts of the setup. Figure 3-6 shows a diagram of this scheme. In the figure, $\Delta\omega$ signifies the detuning that the respective laser beam has.

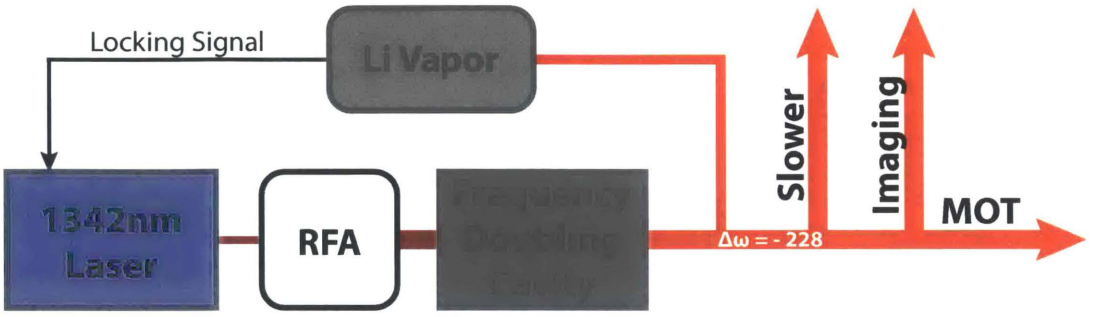

Figure 3-6: Topology of the initial steps in the Laser system. 1342 nm light is amplified and frequency doubled to 671 nm to be used in the Laser system. Some of this light is used to lock the laser to the D_2 line transition of Lithium offset by -228 MHz.

Figure 3-7: Topology of the Slower setup. First offset the whole thing by -772MHz and then using a Double-Pass AOM generate a mized signal with the two needed outputs and send them to the experiment.

3.4.2 Slower

To generate the required outputs, we first use a Double-Pass AOM driven at 386 MHZ to offset the frequency by -772 MHz. This will give us a beam with a total offset of -1 GHz which is what we need for the slower light. However, to generate the repumping light we pass the beam through a 114 MHz driven Double-Pass AOM without blocking the zeroth order light in order to generate a beam that has both a -1GHz component and a -778 MHz component. We then send this beam through a fiber to the experiment. Figure 3-7 shows the topology of this part of the setup.

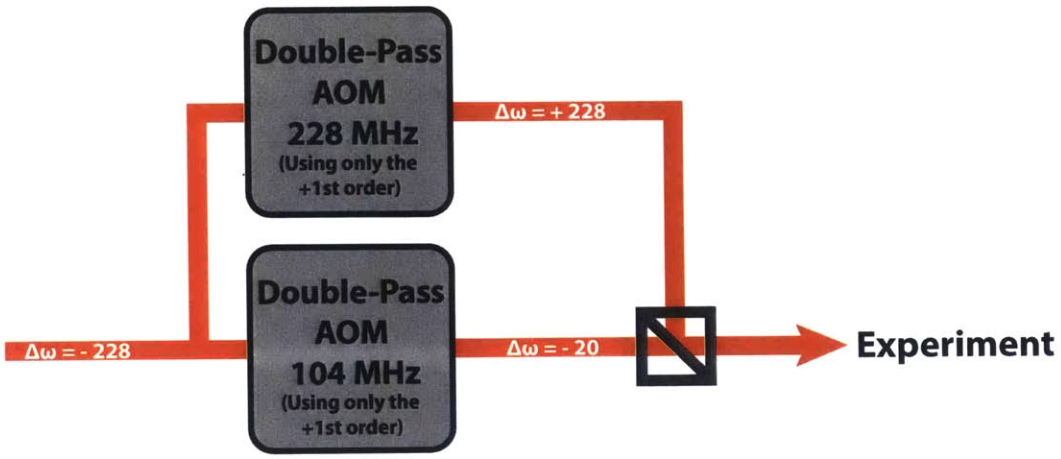

Figure 3-8: Topology of the MOT setup. Using Double Pass AOMs, two separate beams produce the light for the MOT and the MOT Repumper. Then these are mixed in a PBS to be sent to the experiment.

3.4.3 MOT

For the MOT setup, we start by dividing the light into two beams. One will be offset by a 104 MHz driven Double-Pass AOM to get +208 MHz; this will generate a signal -20 MHz from the cycling transition which is red detuned and approximately 3Γ for ^{6}Li. The other beam will be offset by +456 MHz through a Double-Pass AOM driven at 228 MHz to generate a signal at the repumping transition for the MOT Repumper. Both beams are then mixed in a Polarized Beam Splitter so they can be sent together through a fiber to the experiment. Figure 3-8 shows the topology of this part of the setup.

3.4.4 Imaging

The imaging setup is exactly the same as the MOT setup, only this one generates a beam that is resonant with the cycling transition. However, before sending to the experiment there is a 1:1 beam splitter to send the signal divided in two: one for the imaging from the top and one for the imaging from the side. There is also the possibility to send the high-field imaging signal through both outputs. This is done here because the eventual setup that will generate these signals will be closer to the

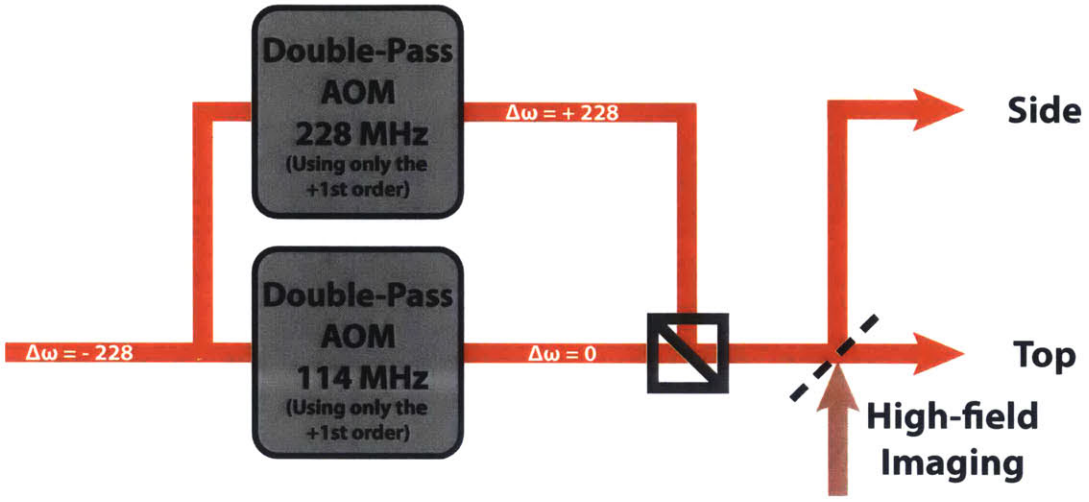

Figure 3-9: Topology of the Imaging setup. The signals are generated exactly the same as the MOT setup. However, now there are two outputs for two different imaging schemes in the experiment: Top and Side. There is also the possibility to send the high-field imaging signal (prepared somewhere else) through the same outputs.

laser system. It will be easier for complexity purposes to be able to send this signal along or instead of the low-field imaging. Figure 3-9 shows the topology of this setup.

3.5 Layout of the Laser System

Finally, Figure 3-10 shows the full layout of the laser system. This figure shows where the main beam is divided towards each part. It is important to mention the amount of beam blocks in the system in order to properly dump the light that is not being used. The figure also shows a simplified layout for the frequency doubling cavity where the 1342 nm light is converted to 671 nm through a non-linear crystal in a bow tie cavity.

A photograph of the finalized laser system is shown in Figure 3-11.

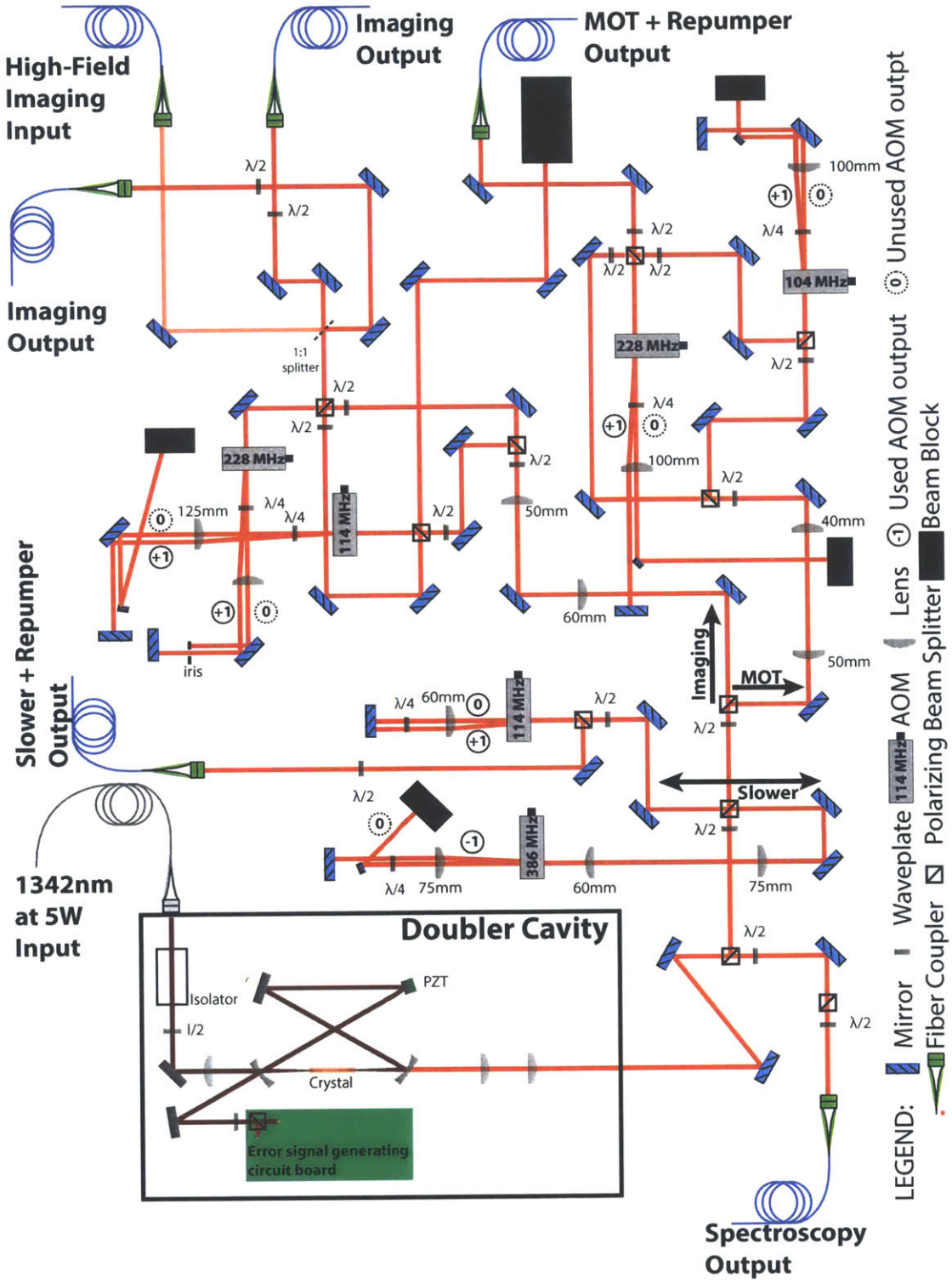

Figure 3-10: Layout of the laser system. The diagram clearly shows how the light is divided and offset to enerate the signals that go to the experiment through polarization-maintaining fibers.

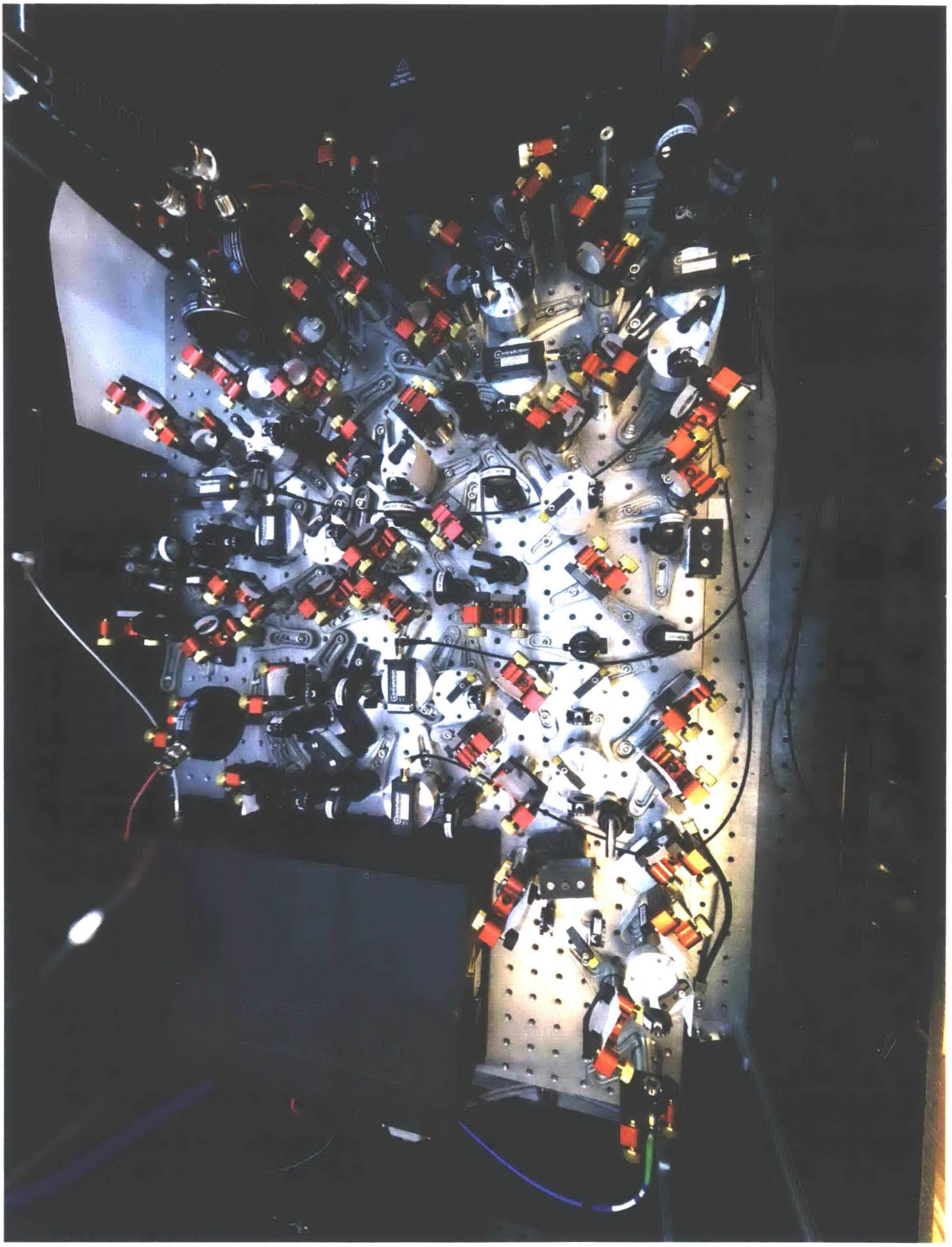

Figure 3-11: Photograph of the laser system. This setup is the same that is displayed in diagram form on Figure 3-10. The big black circles that have a BNC connection are shutters that allow us to mechanically block the light.

Chapter 4

Modulation Transfer Spectroscopy

In this chapter, we will explain how Modulation Transfer Spectroscopy can generate an error signal to lock our laser. The first section will describe the spectroscopy scheme and the theory behind Modulatrion Transfer Spectroscopy. The next section will explain how we implemented this scheme in the experiment and built the spectroscopy setup of which a layout and a photograph is shown. Finally we will talk about locking the laser with the error signal we generated.

4.1 Theory

Spectroscopy is the study of the energy transitions of elements and molecules through the use of light. In its most bare form, it is a technique that looks at the absorption of light through a medium as a function of its frequency. There are many schemes that use this basic principle to generate an error signal that can lock a laser to a specific energy transition. One of these is Modulation Transfer Spectroscopy (MTS).

In this section we will first give an introduction to basic spectroscopic techniques such as Doppler-Free Spectroscopy. Then we will explain the scheme of MTS.

4.1.1 Doppler-Free Spectroscopy

As mentioned before, the most common way to do spectroscopy is by shining a laser beam (light) through an atomic vapor (medium) and measuring the absorption. We can do this measurement by having the beam hit a photodetector that generates an electronic signal proportional to the intensity of the laser beam. If we scan the frequency of the laser beam, we should see a depletion in the photodiode signal whenever the frequency is close to a energy transition in the atom due to the scattering of the light. However, since the atoms are in a gas, they will have a thermal distribution in their velocity centered around 0. This velocity distribution will cause a broadening of the absorption depletion due to the Doppler Shift. In other words, even if the laser is not at the resonant frequency, it can scatter off a velocity group that is Doppler shifted closer to the transition frequency. The shape of the depletion will be gaussian with width kv_{RMS}. The velocity v_{RMS} is defined as $\frac{1}{2}mv_{\mathrm{RMS}}^2 = \frac{3}{2}k_BT$, where m is the mass of the atoms and T the temperature of the cloud.

In order to solve this issue, we employ the Doppler-Free Spectroscopy (DFS) scheme [21]. In this scheme we will send two superimposed and counter-propagating beams through the atom vapor: a "pump" and a "probe". Both beams will have the same frequency and be scanned together; however, we will only measure the intensity of the probe. By doing this, we are circumventing the broadened depletion because the only velocity group that both beams can act on at the same time is the one for which atoms are at rest. Since both beams act on the atoms at rest at the same time, the probe beam will have less absorption due to the atoms being saturated by the pump and leading to peaks exactly at the hyperfine transitions. DFS also generates a peak for "crossover" frequencies because there is a velocity group for which each beam is resonant with a different hyperfine transition still leading to the same saturation of the atoms. Figure 4-1 illustrates the DFS Scheme and the spectroscopy signal that we get for ^{6}Li.

Now that we have a way to get the un-broadened signal for the ^{6}Li cycling transition we need a way to generate an error signal to lock the laser to this.

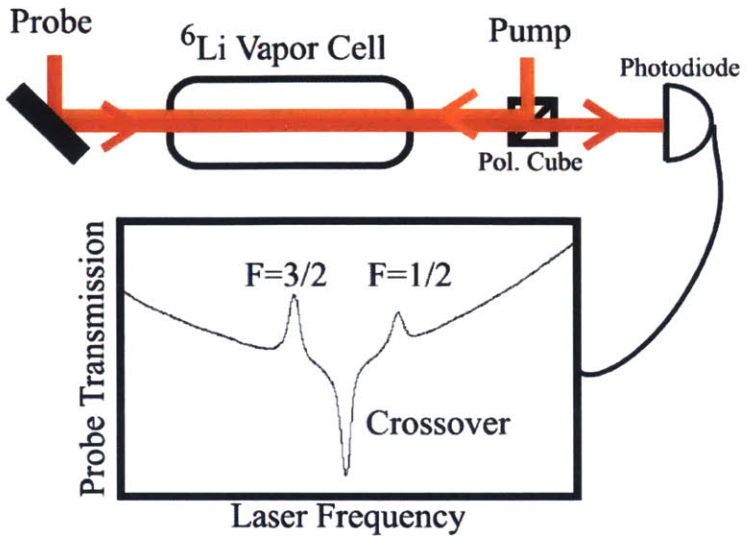

Figure 4-1: Doppler-Free Spectroscopy Scheme for ^{6}Li atoms in the D_2 line transition. Figure taken from [25].

4.1.2 Four-wave mixing

MTS is also referred to as four-wave mixing due to it being a four photon (wave) process [16, 2]. It works by modulating the pump beam so that it carries two sidebands at $\omega_c \pm \omega_m$ where ω_c is the carrier frequency of the pump beam and ω_m the modulation frequency. MTS works by effectively transferring the modulation of the pump beam to the probe beam through a non-linear four photon process (third-order perturbation) only when the carrier frequency is close to a peak in the DFS spectroscopy. MTS has been successfully used before to generate an error signal and lock a laser to a specific spectroscopic line [12, 1].

In this thesis, we will give a brief summary of how MTS produces an error signal based on the calculations made in [12] and [19]. As mentioned before, experimentally we will have the pump beam modulated with sidebands. This modulation can be mathematically expressed as:

$$
\begin{aligned}
E &= E_0 \sin(\omega_c t + \Delta \sin \omega_m t) \\
&= E_0 \left[\sum_{j=0}^{\infty} J_j(\Delta) \sin(\omega_c + n\omega_m)t + \sum_{j=1}^{\infty} (-1)^n J_j(\Delta) \sin(\omega_c - n\omega_m)t \right] \\
&\approx E_0 \left[J_0(\Delta) \sin \omega_c t + J_1(\Delta) (\sin(\omega_c + \omega_m)t - \sin(\omega_c - \omega_m)t) \right] \qquad (4.1)
\end{aligned}
$$

where Δ is the modulation index and $J_n(\Delta)$ the nth-order Bessel function. In reality $\Delta < 1$ so the approximation made in Equation 4.1 its very good. That approximation means having a strong carrier frequency at ω_c and sidebands at $\omega_c \pm \omega_m$.

When passing through the vapor, the pump and probe beam will have a non-linear interaction by which some modulation will appear in the unmodulated probe beam. This is a third-order perturbation theory effect and as such will only be strong at the resonant transitions. This allows us to create a signal that does not depend at all on the background absorption signal. MTS effectively generates a signal that favors the real transitions and "ignores" the crossover peaks due to DFS.

After passing through the vapor and acquiring some of the modulation from the pump beam, the probe beam is shined on a photodiode. The sidebands that the probe beam now has will generate a beat signal that will be measured by the photodiode. This beat signal will have the form:

$$
\begin{aligned}
S(\omega_m) \propto \frac{J_0(\Delta) J_1(\Delta)}{\sqrt{\Gamma^2 + \omega_m^2}} [&(L_{-1} - L_{-1/2} + L_{1/2} - L_1) \cos(\omega_m t + \phi) \\
&+ (D_1 - D_{1/2} - D_{-1/2} + D_{-1}) \sin(\omega_m t + \phi)] \qquad (4.2)
\end{aligned}
$$

Here Γ is the linewidth of the transition, ϕ is a phase difference, and we have the formulas:

$$
L_n = \frac{\Gamma^2}{\Gamma^2 + (\delta - n\omega_m)^2} \text{ and } D_n = \frac{\Gamma(\delta - n\omega_m)}{\Gamma^2 + (\delta - n\omega_m)^2} \qquad (4.3)
$$

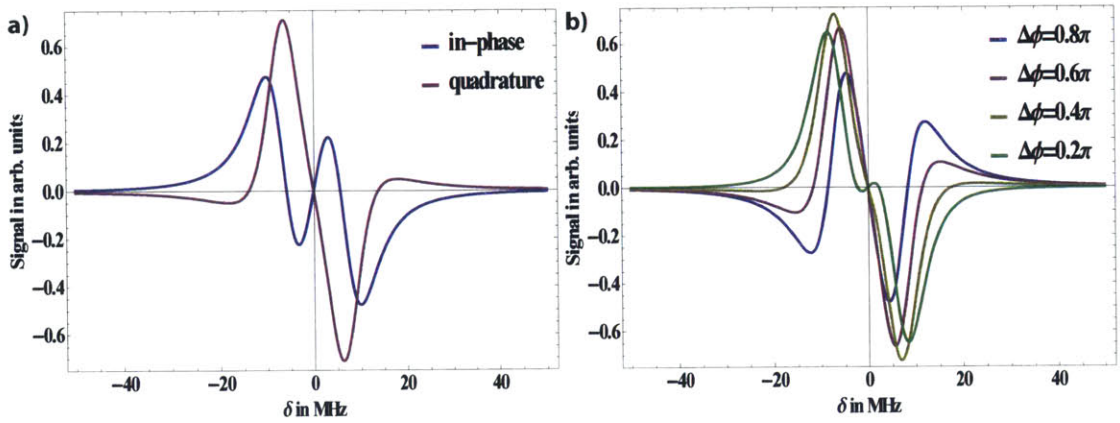

Figure 4-2: Theoretical predictions of the signal generated by Modulation Transfer Spectroscopy in ^{6}Li with Γ =6MHz and ω_m =8.507MHz. a) Shows the quadrature and in-phase components that correspond to the absorption and dispersion components of Doppler Free Spectroscopy respectively. b) Shows the mixture of these signals near the regime that makes a good error signal; the one that results for the best locking signal is $\Delta\phi = 0.6\pi$.

where δ is the detuning of the laser from the transition. In Equation 4.2, the sine term represents the quadrature component of the signal and the cosine term the in-phase component of the signal [12]. By mixing this signal with a wave of frequency ω_m and varying its phase we can recover the absorption and dispersion components of the DFS signal by setting the phase to select the quadrature or the in-phase component respectively [19]. In the end, the best possible error signal will be made by a mixture of both and not only the quadrature or the in-phase terms. Figure 4-2 shows these error signals as predicted by the theory.

As mentioned before, we chose MTS because it generates a very good error signal. A similar scheme to MTS is Frequency Modulation Spectroscopy (FMS) which instead of having the pump modulated, modulates the probe beam and does the same process to get an error signal.

4.2 Implementation

With the theory behind MTS in mind we can finally implement this scheme to generate an error signal to lock the laser on the cycling transition of ^{6}Li. In this section we will first explain the spectroscopy setup that was built and then show its layout. After that we will describe the signal we get as output and how to lock the laser.

4.2.1 Spectroscopy Setup

In Chapter 3, we showed the layout of the laser system which has a small output for the spectroscopy; this is our input for the spectroscopy setup. Before doing the spectroscopy, we offset the light by +228MHz using an AOM driven at 228MHz. This is to have the main beam in the laser system offset by -228MHz as has been mentioned in previous chapters. After this offset, we divide the beam into the probe and pump beams using a PBS. We modulate the pump beam using a home-built EOM[1] driven with a RIGOL DG1022 function generator at 8.507MHz. Next we send both beams in opposite directions through the ^{6}Li vapor cell and we then shine the probe beam into a photodiode. The vapor cell is heated up to 310°C to have a ^{6}Li gas at sufficient pressure in the center of the cell. Figure 4-3 shows the layout of this setup.

It is important to not heat up the vapor cell too much as this will generate the extremes to be hot enough for the Lithium atoms to reach the windows and coat them. This would render the cell unusable. We also built an acrylic enclosure around the cell to minimize the high-temperature effects on the optics. Figure 4-4 shows a photograph of the spectroscopy setup.

4.2.2 Generating the Error Signal

As explained in the past section, we need to mix the signal from the photodiode with a signal at the modulation frequency with a phase offset. We use the RIGOL DG1022 function generator because it has two outputs and it allows to set a phase difference between them. Therefore, we take the photodiode output and amplify it

[1] Appendix A contains the instructions to build this EOM.

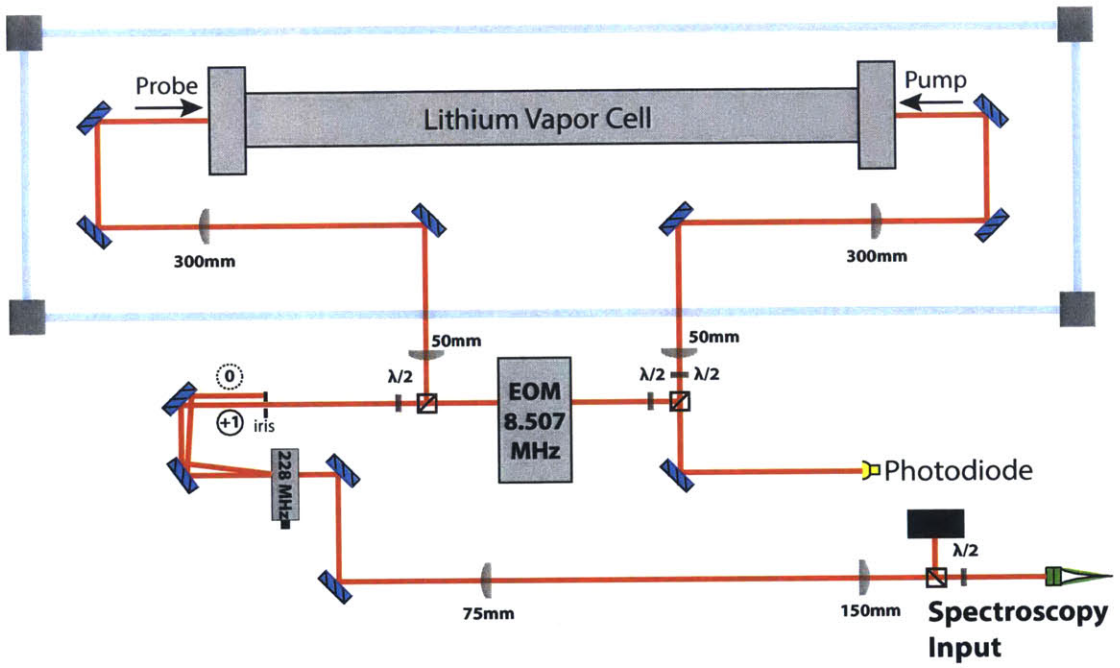

Figure 4-3: Layout of the Spectroscopy Setup. Note the different telescopes that in the setup: the first one is to make the beam smaller and increase the efficiency of the AOM, the other two are meant to expand the beam while it goes through the ^{6}Li gas so that the laser interacts with more atoms. The blue-transparent panes in the layout represent an acrylic enclosure built around the vapor cell so that the heat does not affect the optics outside of it as much.

Figure 4-4: Photograph of the Spectroscopy setup. The white box in the center is the home-built EOM.

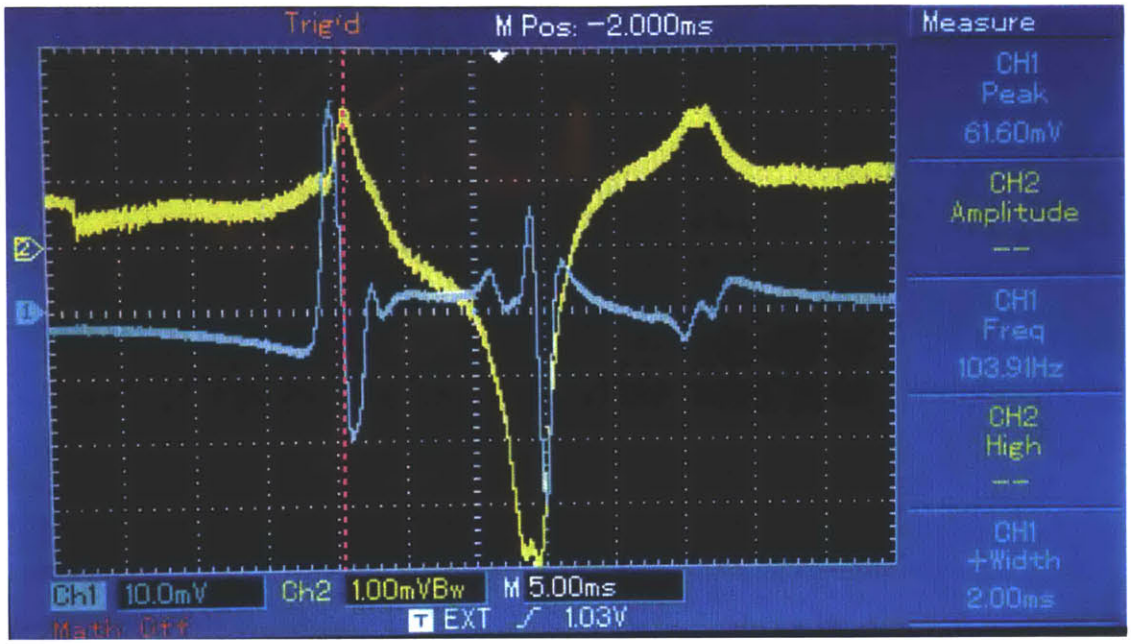

Figure 4-5: Measurement of the error signal generated by our setup. It shows in Yellow the Doppler-Free Spectroscopy signal and in Blue the Modulation Transfer Spectroscopy error signal. Note how the signal for the cycling transition is bigger than that of the crossover.

using a Mini-Circuits^{TM} ZFL-500 amplifier. This signal is then mixed with a 3dBm @ 8.507MHz signal from the function generator in a ZRPD-1+ Phase detector. The output gives us an error signal. Figure 4-5 shows the error signal we got from this setup as measured in an oscilloscope.

4.3 Locking the laser

The error signal is sent to the Toptica PID 110 which locks the laser. Since the laser is dependent on another lock (frequency doubling cavity), the spectroscopy lock will fail if the other one fails. Even though the cavity re-locks very quickly, the spectroscopy signal will be lost because there is no assurance that when the cavity re-locks, the laser will be centered again at the cycling transition. However, since the cavity can be tuned to not unlock very easily this will not be a problem when the experiment is running.

Appendix A

Building an Electro-Optic Modulator

In this appendix we will describe how to build the Electro-Optic Modulator (EOM) that was used to do Modulation Transfer Spectroscopy. We will first explain what composes an EOM. Then give a list of the materials needed to build the EOM. Finally we will describe how to test and search for the resonant frequencies of the EOM.

A.1 How does an EOM work?

An EOM modulates a laser beam through a non-linear effect inside a birefringent crystal that has an oscillating electric field through its main axis. For the effect to be strong enough we need a very strong electric field. To get this, we use the principle of tank circuits: If we have an inductance L and a capacitance C in an AC circuit, this will have a resonant frequency at $2\pi f_{res} = 1/\sqrt{LC}$. At this resonance, the effective resistance of the circuit is 0 and therefore the current grows asymptotically. This causes the electric field inside the capacitor to oscillate with an asymptotic maximum value. Therefore an EOM is a tank circuit where the crystal is in-between two parallel plates making the capacitance. The values of the sidebands it creates were already presented in Chapter 4.

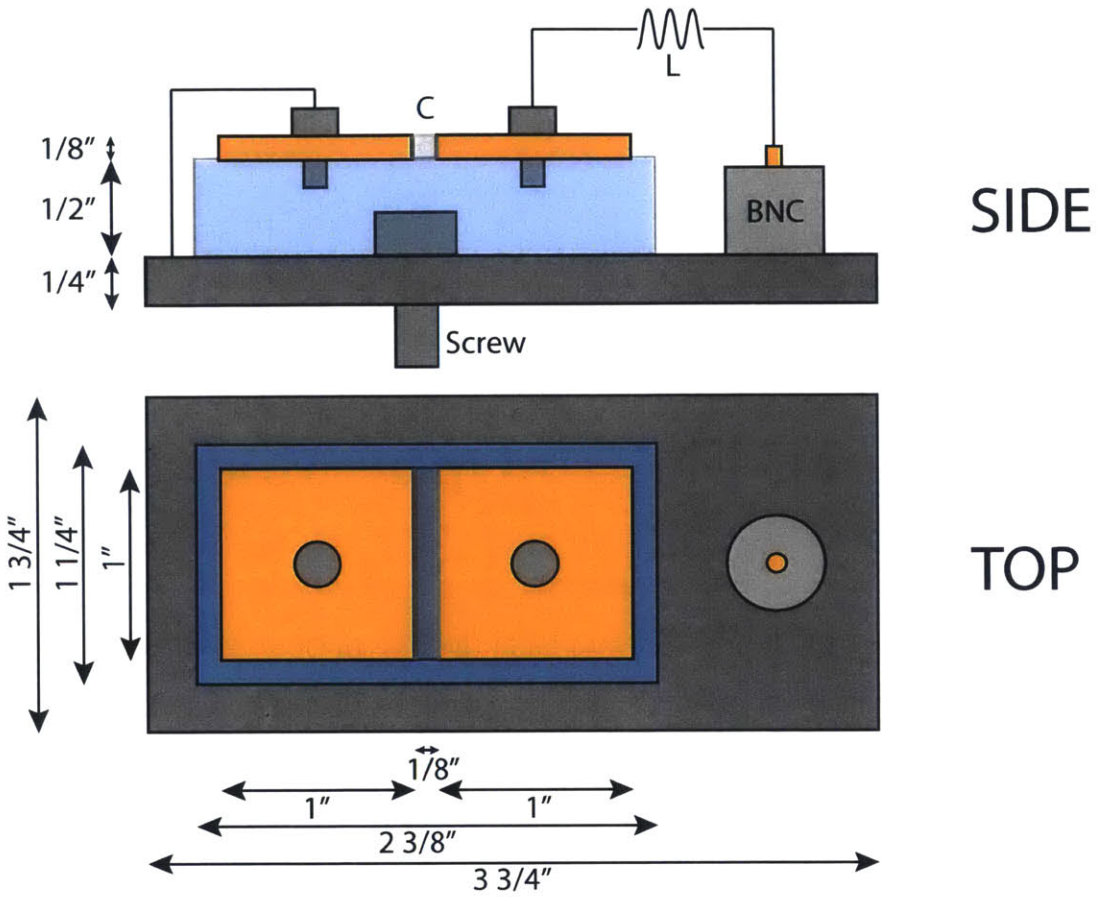

Figure A-1: Design of the home-build EOM at scale 1:1. The output of the BNC is not specifically right, but illustrates how the EOM works.

A.2 How to build the EOM?

The EOM that was built for this laser system was based on the one described in [12]. The main part we need is an EOM crystal, in this case we use a $LiNbO_3$ (lithium niobate) crystal 1" long and square cross-section of side 1/8". We also need a set of choke inductors (RF inductors) so that we can try many until we get the resonance we want (In the one that was built we ended up using an $L = 22\mu H$). Apart from that we use a BNC connector, Indium foil, and some raw material: brass, aluminum, and acrylic. The specific sizes of the materials will be shown in the design. Figure A-1 shows the design of the home-built EOM.

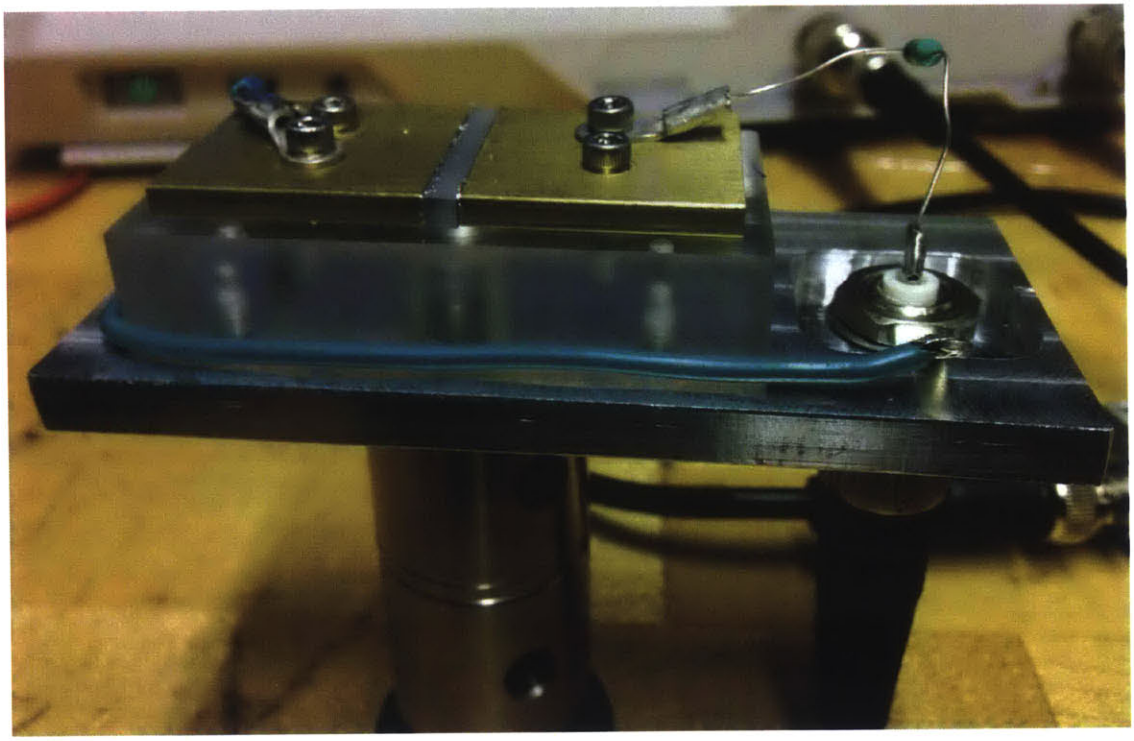

Figure A-2: Photograph of the home-build EOM for the Modulation Transfer Spectroscopy.

Not very clear in the design is that the Indium foil is placed at the contact of the EOM crystal and the brass plates to maximize the electrical contact. A photograph of the built EOM is shown in Figure A-2. It does not show the cover that appears in Figure 4-4, this was simply milled out of a block of white plastic so that it could sit on top of the EOM and protect the crystal from dust.

A.3 How to test the resonance of the EOM?

For this, we first need a Spectrum Analyzer that has a Local Oscillator (LO) such as the RIGOL DSA 815. We connected the LO output of the spectrum analyzer to the output of a coupler (any coupler will work, just search for a MiniCircuits^{TM} laying around). Next, we connected the input to the coupler to the EOM, and the input of the spectrum analyzer to the CPL output of the coupler. In the Spectrum Analyzer we

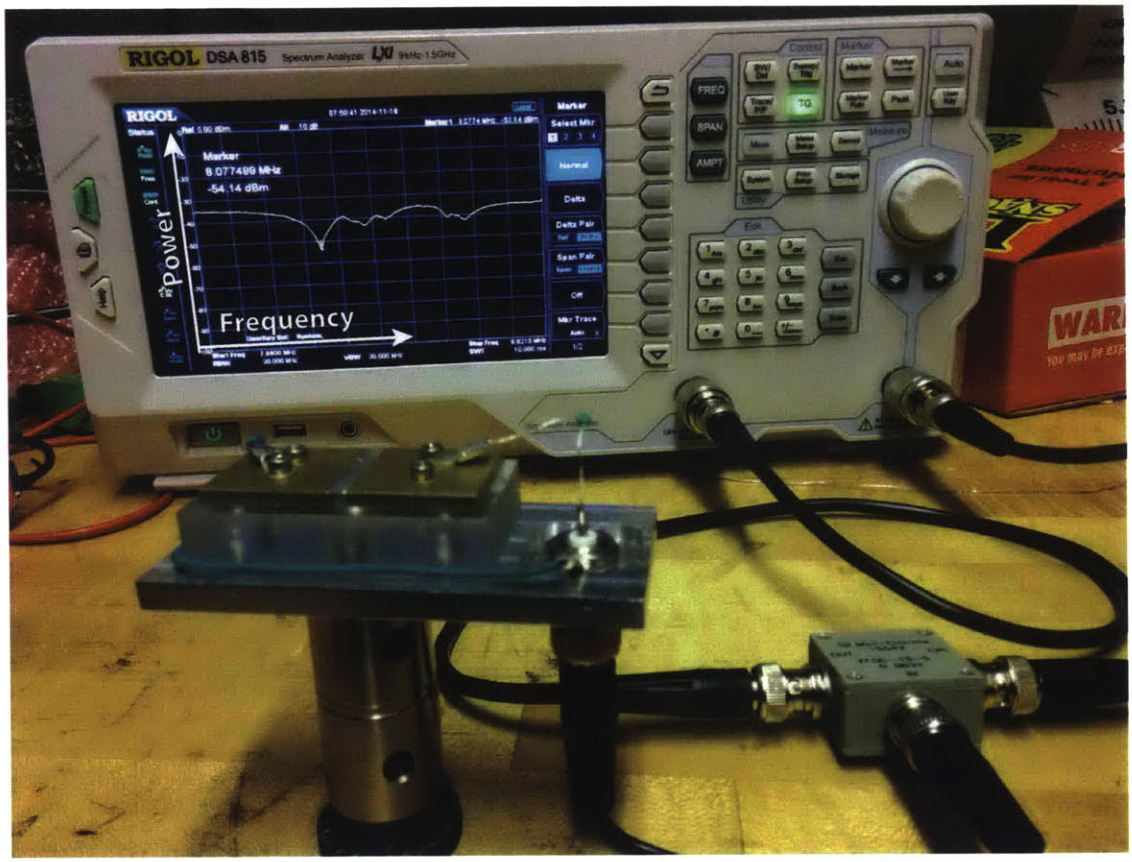

Figure A-3: Photograph of the testing scheme for the resonances of the EOM. There is a very clear depletion at 8.077 MHz and several more. In this picture, there is a small but very sharp depletion at 8.507 MHz which is the frequency we ended up using.

chose the Tracking Generation (TG) option and set the scan to the region of interest. Alternatively, one could simply use a Network Analyzer if available. In our case, we wanted a value that was bigger than Γ but not too much because that is where MTS gives good error signals. The screen shows now a line with some depletions that correspond to resonances. We tested many different choke inductors until we saw a signal around the desired frequency. It is desired to see a sharp depletion, this means that the resonance has a big Q-factor which is what defines how strong it is. Figure A-3 shows a picture of this test taking place. This initial test serves mainly to choose a choke inductor for the EOM.

After this, we made a more sophisticated test by building an interferometer where

we passed one of the beams through the EOM and the other one shifted by an AOM. After recombining both beams we combined them on a photodiode and saw three peaks on a spectrum analyzer: one due to the beat signal of the carrier frequency and the shifted one, and the other two by the sidebands. A strong resonance at the EOM generates a stronger signal for the sidebands. Then we tuned the frequency driving the EOM and measured the strength of the sidebands with the spectrum analyzer. This to find the frequencies at which the sidebands were the strongest. This is a slightly more complicated test but one that gives more reliable data. It was with this test that we realized there was another very good resonance at 8.507 MHz.

Finally, the ultimate test is actually using the EOM in the spectroscopy setup. We modified the frequency slightly around the resonances that we had found until we maximized the error signal generated.

Bibliography

[1] F. Bertinetto, P. Cordiale, G. Galzerano, and E. Bava. Frequency stabilization of dbr diode laser against cs absorption lines at 852 nm using the modulation transfer method. *IEEE Trans. Instrum. Meas.*, 50, 2001.

[2] D. Bloch, R. K. Raj, K. S. Peng, and M. Ducloy. Dispersive character and directional anisotropy of saturated susceptibilities in resonant backward four-wave mixing. *Phys. Rev. Lett.*, 49:719–722, Sep 1982.

[3] N. Bloembergen and P. S. Pershan. Light waves at the boundary of nonlinear media. *Phys. Rev.*, 128:606–622, Oct 1962.

[4] Simone Donadello, Simone Serafini, Marek Tylutki, Lev P. Pitaevskii, Franco Dalfovo, Giacomo Lamporesi, and Gabriele Ferrari. Observation of solitonic vortices in bose-einstein condensates. *Phys. Rev. Lett.*, 113:065302, Aug 2014.

[5] C. Foot. *Atomic Physics.* Oxford University Press, 2005.

[6] P. A. Franken, A. E. Hill, C. W. Peters, and G. Weinreich. Generation of optical harmonics. *Phys. Rev. Lett.*, 7:118–119, Aug 1961.

[7] M. E. Gehm. *Preparation of an optically-trapped degenerate Fermi gas of 6Li: finding the route to degeneracy.* PhD thesis, Duke University, 2003.

[8] Metcalf H. and van der Straten P. *Laser Cooling and Trapping.* Springer, 1999.

[9] Z. Hadzibabic. *Studies of a Quantum Degenerate Fermionic Lithium Gas.* Ph.d. thesis, Massachusetts Institute of Technology, 2003.

[10] M. J.H. Ku, W. Ji, B. Mukherjee, E. Guardado-Sanchez, L. W. Cheuk, T. Yefsah, and M. W. Zwierlein. Motion of a solitonic vortex in the bec-bcs crossover. *Phys. Rev. Lett.*, 113:065301, Aug 2014.

[11] Giacomo Lamporesi, Simone Donadello, Simone Serafini, and Gabriele Ferrari. Compact high-flux source of cold sodium atoms. *Rev. Sci. Instrum.*, 84, 2013.

[12] D. J. McCarron, S. A. King, and S. L. Cornish. Modulation transfer spectroscopy in atomic rubidium. *Meas. Sci. Technol.*, 19, 2008.

[13] D. Moravchik. *Imaging methods of cold atoms.* Master thesis, Ben-Gurion University of the Negev, 2009.

[14] William D Phillips. Laser cooling and trapping of neutral atoms. Technical report, DTIC Document, 1992.

[15] E. L. Raab, M. Prentiss, Alex Cable, Steven Chu, and D. E. Pritchard. Trapping of neutral sodium atoms with radiation pressure. *Phys. Rev. Lett.*, 59:2631–2634, Dec 1987.

[16] R. K. Raj, D. Bloch, J. J. Snyder, G. Camy, and M. Ducloy. High-frequency optically heterodyned saturation spectroscopy via resonant degenerate four-wave mixing. *Phys. Rev. Lett.*, 44:1251–1254, May 1980.

[17] V. Ramasesh. *Towards a Quantum Gas Microscope for Fermionic Atoms*. Undergraduate thesis, Massachusetts Institute of Technology, 2012.

[18] Ibon Santiago Gonzalez. *LiNaK: Multi-Species Apparatus for the Study of Ultracold Quantum Degenerate Mixtures*. Master thesis, Massachusetts Institute of Technology, 2008.

[19] J. H. Shirley. Modulation transfer processes in optical heterodyne saturation spectroscopy. *Opt. Lett.*, 7, 1982.

[20] J. C. White. Stimulated raman scattering. In L. F. Mollenauer and J. C. White, editors, *Tunable Lasers*, volume 59 of *Topics in Applied Physics*, pages 115–207. Springer Berlin Heidelberg, 1987.

[21] C. Wieman and T. W. Hänsch. Doppler-free laser polarization spectroscopy. *Phys. Rev. Lett.*, 36:1170–1173, May 1976.

[22] Feng Y., S. Huang, A. Shirakawa, and K.I. Ueda. 589 nm light source based on raman fiber laser. *Jap. Jour. App. Phys.*, 43, 2004.

[23] T. Yefsah, A. T. Sommer, M. J.H. Ku, L. W. Cheuk, W. Ji, W. S. Bakr, and M. W. Zwierlein. Heavy solitons in a fermionic superfluid. *Nature*, 499:426–430, Jul 2013.

[24] M. W. Zwierlein, J. R. Abo-Shaeer, A. Schirotzek, C. H. Schuck, and W. Ketterle. Vortices and superfluidity in a strongly interacting fermi gas. *Nature*, 435:1047–1051, Jun 2005.

[25] Martin Zwierlein. Cooling and trapping a bose-fermi mixture of dilute atomic gases. *Undergraduate Thesis*, 2001.